Science of the Total Environment 836 (2022) 155694

Contents lists available at ScienceDirect

Science of the Total Environment

journal homepage: www.elsevier.com/locate/scitotenv

Contamination and source-specific risk analysis of soil heavy metals in a typical coal industrial city, central China

Xian-Meng Shi [a,b,1], Shuai Liu [c,1], Liang Song [a,d,*], Chuan-Sheng Wu [e], Bin Yang [a], Hua-Zheng Lu [a], Xun Wang [f], Sissou Zakari [g]

[a] CAS Key Laboratory of Tropical Forest Ecology, Xishuangbanna Tropical Botanical Garden, Chinese Academy of Sciences, Yunnan 666303, China
[b] College of Biology and Food, Shangqiu Normal University, Henan 476000, China
[c] School of Ecology and Environment, Anhui Normal University, Anhui 241000, China
[d] Ailaoshan Station for Subtropical Forest Ecosystem Studies, Xishuangbanna Tropical Botanical Garden, Chinese Academy of Sciences, Jingdong, Yunnan 676209, China
[e] Anhui Province Key Laboratory of Environmental Hormone and Reproduction, Fuyang Normal University, Anhui 236037, China
[f] State Key Laboratory of Environmental Geochemistry, Institute of Geochemistry, Chinese Academy of Sciences, Guiyang 550081, China
[g] Laboratory of Hydraulics and Environmental Modeling, Faculté d'Agronomie, Université de Parakou, Parakou 03 BP 351, Benin

HIGHLIGHTS

- Moderate soil contamination by Cd and Hg is identified in the study area.
- Source-specific risks are apportioned using PMF-based risk assessment methods.
- The source profiles of potential ecological risks vary in urban and suburban areas.
- Human health risks posed by soil HMs are mainly from traffic and natural sources.

GRAPHICAL ABSTRACT

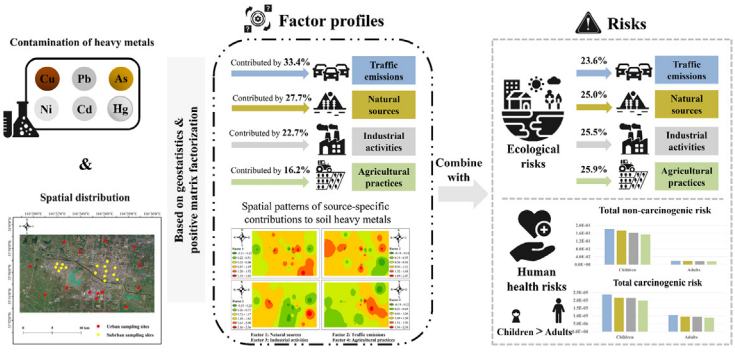

ARTICLE INFO

Editor: Xinbin Feng

Keywords:
Soil pollution
Source apportionment
Coal-mining
Ecological risk
Human health risk

ABSTRACT

Source-specific risk apportionment for soil heavy metals (HMs) is crucial for pollution mitigation and risk control in coal-mining areas. The ecological and human health risks resulting from different sources were evaluated through an integrated method that combines risk assessments with positive matrix factorization (PMF) model. Thirty soil samples were collected from a typical coal-mining city in central China and analyzed for six HMs (Cu, Ni, Pb, Cd, As, and Hg). The results indicate that surface soil in the study area suffered from moderate HMs pollution, especially pollution by Cd and Hg. Four potential sources of soil HMs were identified and quantified in the study area, including natural source (27.7%), traffic emissions (33.4%), agricultural practices (16.2%), and industrial activities (22.7%). The ecological risk of the study area was at moderate level, and the leading contributions in urban and suburban areas were from industrial activities and agricultural practices, respectively. The non-carcinogenic risks for adults and children were lower than the risk threshold, while the carcinogenic risks ranged between 1E−06 and 1E−04, suggesting that carcinogenic risks and hazards to human health should not be neglected. Traffic emissions and natural sources mainly contributed to the non-carcinogenic and carcinogenic risks, due to the strong non-carcinogenicity and carcinogenicity of As and Ni. These findings highlight the ecological and health risks linked to potential sources of soil HMs contamination and provide valuable information on the reduction of corresponding risks for local environmental managers.

* Corresponding author at: CAS Key Laboratory of Tropical Forest Ecology, Xishuangbanna Tropical Botanical Garden, Chinese Academy of Sciences, Yunnan 666303, China.
E-mail address: songliang@xtbg.ac.cn (L. Song).
[1] Both authors contribute equally to this work.

http://dx.doi.org/10.1016/j.scitotenv.2022.155694
Received 9 January 2022; Received in revised form 17 April 2022; Accepted 30 April 2022
Available online 4 May 2022

1. Introduction

Coal mining activities can cause serious environmental pollution because large amounts of heavy metals (HMs) are released into the surrounding areas (Li et al., 2014; Sun et al., 2019; Cheng et al., 2020). Several studies reported that airborne particles (Ren et al., 2021), road dust (Cui et al., 2020), water (Mahato et al., 2017), sediment (Ji et al., 2017), soil (Cheng et al., 2020), and crops (Hossen et al., 2021) are contaminated with HMs in coal mining areas. The presence of high HMs contents in soils can damage soil ecosystems, reduce soil biological communities, cause toxic effects on plants, and reduce agricultural productivities (Huang et al., 2019; Liu et al., 2020). Concerns on the ecological and human health risks presented by HMs pollution are growing from both academia and the public, because of their high toxicity, persistence and accumulation (Han et al., 2020; Jiang et al., 2020). In fact, a continuous retention of HMs in the environment can cause chronic toxicity for human, causing damage to nervous system, blood composition, kidneys, lungs, liver and even death (Tchounwou et al., 2012; Gu and Gao, 2018; Briffa et al., 2020). Therefore, from the viewpoint of environment and human health protection, it is important to evaluate the contamination levels and primary sources of soil HMs in typical areas with intensive coal-mining activities.

The quantification of soil HMs originating from natural or anthropogenic sources is vital for understanding and analyzing priority contaminants (Jiang et al., 2020; Men et al., 2020). Based on the constraints conditions, positive matrix factorization (PMF) model is widely utilized in many regions for the apportionment of contaminants source in the environmental medias (Men et al., 2020; Heidari et al., 2021; Huang et al., 2021; Luo et al., 2022). Indeed, source profiles are not required in PMF, while each data point is weighed based on its uncertainty (Jiang et al., 2017). The results of PMF provide an important basis for the assessment and control of pollution (Huang et al., 2018; Luo et al., 2022). Moreover, the results of source apportionment do not provide information about human health risks associated with these sources of contamination (Guo et al., 2021). It has been demonstrated that soil HMs from anthropogenic or natural sources contain different fractions associated with human health risks (Lei et al., 2010; Cao et al., 2018); thus, source-specific risk evaluation can be the precursor to identify priority sources.

Several factors can affect risks associated with HMs including concentration, toxicity and the integrative actions of multiple types of HMs (Jiang et al., 2020; Men et al., 2020). Thus, the assessment of risks and contamination caused by HMs have been performed using various methods, among which geo-accumulation index (I_{geo}), pollution index (PI), and pollution load index (PLI) have been widely used to compute the contamination status of soil HMs (Men et al., 2018, 2020; Huang et al., 2021; Luo et al., 2022). Meanwhile, the potential ecological risk index (RI) and human health risk (HHR) evaluation methods are used to assess the threats of HMs to the environment and human health, respectively (Jiang et al., 2020; Heidari et al., 2021). These classic methods can provide accurate information regarding HMs pollution levels, but do not target the quantitative distribution of the sources of pollutants (Men et al., 2020). Nevertheless, quantitative risk apportionment is essential and beneficial to prevent contamination and to control the risks of soil HMs. Therefore, an integrated approach that couples source apportionment with risk assessment models was performed to obtain source-specific risk estimates in this study (Jiang et al., 2020; Men et al., 2020). This method helps to quantify ecological and human health risks from various sources, so that the priority pollution sources can be determined, and effective measures can be taken to protect the ecosystem and human health (Jiang et al., 2020).

Previous studies have indicated that soil HMs contaminating the surrounding of mining areas mainly emanate from industrial emissions (Li et al., 2014; Liu et al., 2019; Sun et al., 2019), such as coal mining and smelting activities; but research on the quantification of specific risks from various sources is still lacking. Considering the high contributions of coal-mining activities to soil HMs concentrations, we thus hypothesized that the ecological and human health risks are mainly from the anthropogenic source of coal-related industrial activities. Taking a typical coal industrial city from central China, Yongcheng, as an example, a comprehensive approach was used to quantify the ecological and human health risks of soil HMs from different sources. The city possesses rich coal mine resources with an underground storage area of 1326 km^2, and is one of the seven largest coal chemical bases across the nation (Lu et al., 2020). Therefore, the current pollution status and apportion risk sources of soil HMs were evaluated using geostatistics and PMF-based risk assessment methods. The objectives of this research are: (1) to explore the contamination levels of soil HMs, (2) to identify and apportion the potential sources of soil HMs contamination, and (3) to quantify the source-specific ecological and human health risks posed by soil HMs in the study area. The results of this research will provide effective information on the quantification of priority contamination sources, and will be of great importance to prevent further ecological and health risks in typical coal industrial cities.

2. Materials and methods

2.1. Study area

This study is performed in the core areas of the Yongcheng city (ca. 300 km^2), eastern Henan Province (33°42′–34°18′N, 115°58′–116°39′E). The total administrative area of Yongcheng is 2020 km^2, including 2000 km^2 of plain area with a total population of about 1.6 million (Lu et al., 2020). The city falls in the sub-humid zone of warm temperate zone, where monsoon has a significant impact. The annual average temperature and precipitation are 14.4 °C and 868 mm, respectively. The city has fluvio-aquic and lime concretion black soil types, with relatively low organic matter content (Lu et al., 2020).

2.2. Sample collection and analysis

The sampling area was divided into urban area with high resident density, and suburban area dominated by industrial and agricultural activities (Fig. 1). A total of 30 soil samples were collected from surface soil (0–20 cm) in August 2020, consisting of 16 samples in the urban area and 14 samples in the suburban area (Fig. 1). For each sampling site (10 m × 10 m), five subsamples were collected from five spots and mixed to obtain a composite fresh soil sample of about 1.5 kg (Sun et al., 2019). The collected soil samples were stored in self-sealing polyethylene bags and immediately transported to the laboratory (Cheng et al., 2020). The specific location of each sampling site was recorded as global positioning system (GPS) coordinates (Cheng et al., 2020). After air-drying for 15 days, the soil samples were then sieved through a 1000-μm nylon mesh to remove debris (Men et al., 2020), and carefully stored in airtight polyethylene bags in a refrigerator at <4 °C prior to analysis.

Six HMs were measured, namely Cu, Ni, Pb, Cd, As, and Hg, which typically coexisted in the soil of the study area. Approximately 100 mg of homogenized soil sample was put in a Teflon digestion container, and digested using HNO_3-$HClO_4$-HF in a microwave. The digested solution was cooled, filtered and diluted to 25 ml. Then after, the concentrations of Cu, Ni, Pb, and Cd were measured by inductively coupled plasma–mass spectrometry method (ICP–MS, Thermo Fisher, USA), and the concentrations of As and Hg were determined using atomic fluorescence spectrometry method (AFS-SA20, Jitian Ltd., China). Reagent blanks, replicated samples, and standard reference materials were used to provide quality assurance and control (QA/QC), and the recoveries of these HMs were in the range of 93% and 115%. The method detection limits of Cu, Ni, Pb, Cd, As, and Hg were 1, 1, 0.1, 0.01, 0.01 and 0.002 mg kg^{-1}, respectively. The relative standard deviations (RSDs) of the duplicated samples were less than 5%.

2.3. Contamination status

The contamination levels of soil HMs were evaluated using indices including pollution index (PI), pollution load index (PLI), and geo-

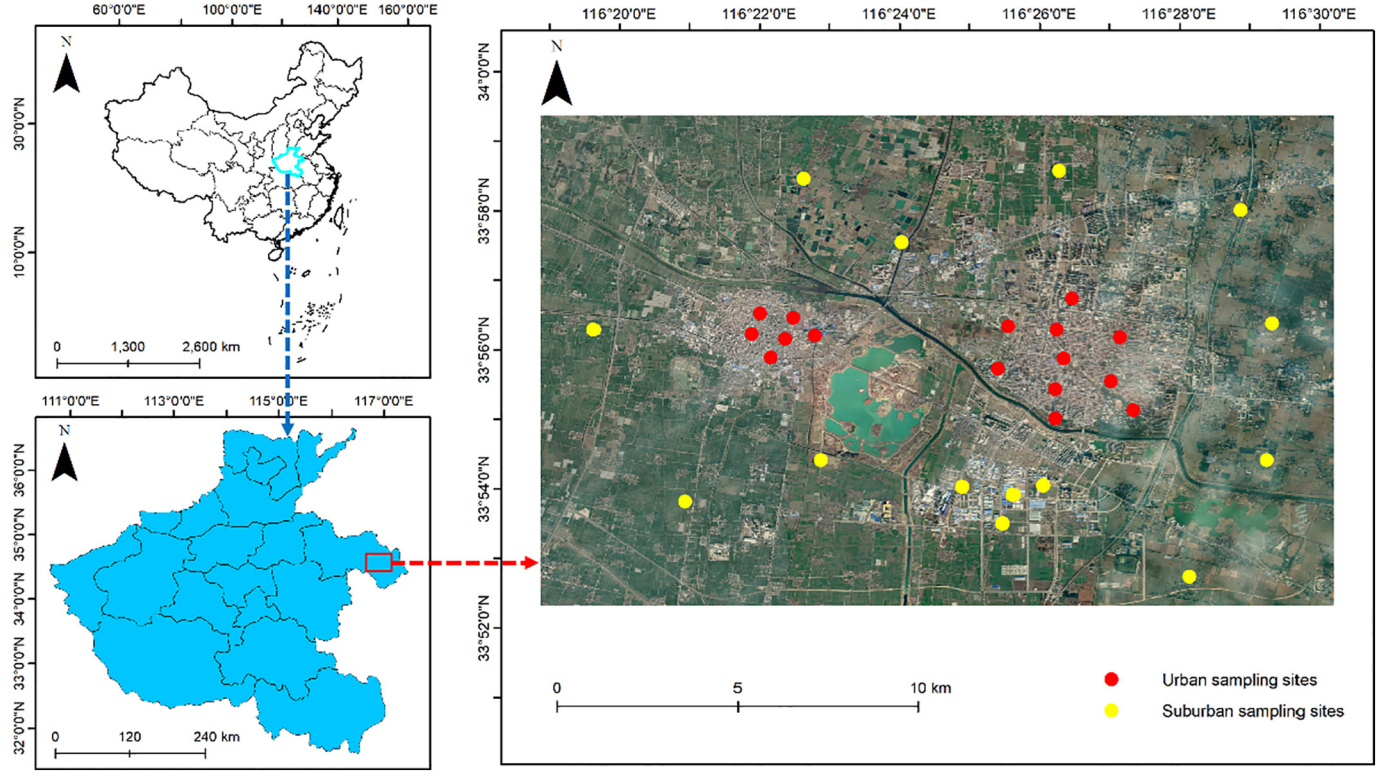

Fig. 1. Maps of study area and sampling sites.

accumulation index (I_{geo}). PI represents the pollution level with a single HM and PLI reflects the overall pollution level of all HMs in a soil sample. PI and PLI were calculated based on each soil sample, and are determined using the following equations (Wang et al., 2021; Luo et al., 2022):

$$\mathrm{PI} = \frac{C_i}{B_i} \tag{1}$$

$$PLI = (PI_1 \times PI_2 \times PI_3 \times \cdots\cdots \times PI_n)^{1/n} \tag{2}$$

where C_i represents the measured concentration of HM_i, B_i denotes its corresponding background value (BV) in Henan Province (CNEMC, 1990), and n is the number of HMs. The classification of HMs contamination in soils based on PLI is listed in Table S1.

Geo-accumulation index (I_{geo}) is the most popular index used to assess the contamination level of HMs in soil samples, and to compare the present and background concentrations of the same area (Men et al., 2018). The I_{geo} was calculated as:

$$I_{geo} = \log_2\left[\frac{C_i}{1.5 \times B_i}\right] \tag{3}$$

here, C_i and B_i are the contents of HM in each sample and its corresponding BV, respectively. The coefficient 1.5 is generally used to regulate the anthropogenic impacts (Huang et al., 2021). The pollution levels of HMs according to the ranges of I_{geo} are given in Table S1.

2.4. Source apportionment

The PMF model developed by the USEPA was applied to apportion the sources of soil HMs. The model decomposed a matrix sample data into factor contribution and factor profiles under non-negative limits (USEPA, 2014). The model helps to solve origin profiles and origin contributions according to synthetic datasets (Guan et al., 2018; Jiang et al., 2020). The species concentrations and uncertainty associated with the sample species data were used to weight individual points in the model (USEPA, 2014). The uncertainty was either a sample-specific or equation-based uncertainty (Guo et al., 2021). Per Huang et al. (2018), the uncertainty of each sample was calculated using the equation-based uncertainty profile in this study (see Supporting information S1).

As well, statistical analysis of geographical data was used to intuitively reflect local conditions, which proved an effective method to identify pollution hotspots and determine their sources (Zhang et al., 2018; Cheng et al., 2020; Luo et al., 2022). The spatial analyses of soil HMs were conducted as a confirmation of source apportionment, using the Inverse Distance Weighting (IDW) method in ArcGIS version 10.7 (Fig. S1).

2.5. Source-specific risk analysis

2.5.1. PMF-based RI model

The potential ecological risk index (RI) was computed to assess the degree of ecological risk related to soil HMs. The PMF-based RI model is a new integrated method to quantify the ecological risks of soil HMs from different sources (Heidari et al., 2021; Wang et al., 2021). In the present study, the contribution of each source (factor) was calculated using procedure described in Jiang et al. (2020). In short, the mass concentration of pollutant n in sample j originated from source l (C_{jn}^{l}) was first calculated by the following equation:

$$C_{jn}^{l} = *C_{jn}^{l} \times C_j \tag{4}$$

where $*C_{jn}^{l}$ is the calculated concentrations (mg kg^{-1}) of soil HM n from source l in sample j, and C_j is the concentrations of soil HMs in sample j (Jiang et al., 2020).

Then, the total concentration of soil HMs to RI originated from various sources was quantified. The calculation of ecological risk posed by soil HMs from source l in sample j (RI_j^l) is given as:

$$RI_j^l = \left(\sum E_r^i\right)_j^l = \sum \frac{C_{jn}^{l}}{B_i} \times T_r^i \tag{5}$$

where E_r^i and T_r^irefer to the potential ecological risk and the toxicity coefficient of HM_i, respectively. B_i is the background value of HM_i. The values of T_r^i for Cu, Ni, Pb, Cd, As, and Hg are 5, 5, 1, 30, 10, and 40, respectively (Norris et al., 2014; Luo et al., 2022). The categorization of ecological risk levels based on E_r^i and RI values is given in Table S2.

2.5.2. PMF-based HHR model

The exposure to health risks were calculated using the average daily intake (ADI) of soil HMs through three pathways: direct ingestion, inhalation, and dermal contact absorption. Considering the behavioral and physiological differences between children and adults, they were divided into two groups and assessed separately (Sun et al., 2019). An integrated approach (PMF-based HHR model) combining the HHR with PMF was applied to assess the contribution of each source to the total health risk. The first step was to import the contributions of HMs in each soil sample from each source into the HHR formula. Thereafter, we quantitatively evaluated the non-carcinogenic and carcinogenic risks posed by HMs from each source (Jiang et al., 2020; Wang et al., 2021). Detailed calculation of ADI and related indexes in the formulas is provided in the Supporting information S2 and Table S3.

Non-carcinogenic risk from HMs is expressed by the hazard quotient (HQ_i), which is calculated with respect to the ADI of each HM and the corresponding reference dose (R_fD) (Jiang et al., 2020). Here, $HQ_{jn}{}^{l}{}_{i}$ is the hazard quotient for the exposure route i (ingestion, inhalation or dermal absorption) from source l of the HM n in sample j. The total hazard index (THI) is calculated as:

$$\mathrm{HI} = \sum HQ^{l}_{jn_i} = \sum \frac{ADI^{l}_{jn_i}}{\mathrm{RfD_i}} \tag{6}$$

$$\mathrm{THI} = \sum HI \tag{7}$$

here, if the value of HI > 1, it indicates that soil HMs may pose adverse health risk; if HI < 1, it means that the non-carcinogenic risk is insignificant (Huang et al., 2021).

The carcinogenic risk (CR_i) is calculated by multiplying the ADI by the slope factor (SF_i). Here, $CR_{jn}{}^{l}{}_{i}$ is the carcinogenic risk for the exposure route i from source l of the HM n in sample j (Jiang et al., 2020). As with THI, the total CR_i (TCR) is calculated as:

$$\mathrm{CR} = \sum CR^{l}_{jn_i} = \sum ADI^{l}_{jn_i} \times \mathrm{SF_i} \tag{8}$$

$$\mathrm{TCR} = \sum CR \tag{9}$$

where the precautionary criterion is 1E−06, which indicates that one per million people suffer from excess risks. The cautionary criterion of 1E−04 demonstrates that people suffers from significant risks of cancer (Men et al., 2021; Luo et al., 2022). The corresponding parameter values used in above formulas were summarized in Tables S3–S4.

3. Results and discussion

3.1. Concentrations of soil heavy metals

The descriptive statistics of soil HMs concentrations in the study areas are shown in Table 1. The average concentrations of six HMs in Yongcheng were higher than the BVs of Henan Province (CNEMC, 1990), especially Cd and Hg, which were 1.76 and 2.24 times higher compared to their BVs, respectively. This finding subsequently confirms that the concentrations of Cd and Hg were strongly disturbed by anthropogenic activities (Huang et al., 2021; Wang et al., 2021). The mean soil HMs concentrations were higher in urban area than in suburban area, indicating significant contributions from residential activities and traffic emissions to the accumulations of HMs in urban area. As a result, the soils in urban and suburban areas of Yongcheng were differently contaminated with HMs.

The coefficient of variation (CV) of Hg exceeded 50%, indicating a strong variation of this heavy metal and its strong interference with external factors (Jiang et al., 2020). Point source pollution occurred in Hg distribution, revealed by the detection of extremely high Hg concentrations in some samples from the agricultural areas (Fig. S1). In contrast, the CVs of the other HMs were less than 25%, suggesting a slight variation in these HMs (Wang et al., 2021). The study area is a typical coal industrial city, where the most obvious sources of interference are transportation and coal-related industrial activities. Different types of HMs have been emitted from these human activities and scattered in various media (Cheng et al., 2020). The HMs enter the atmosphere and settle in various places as the air flows (Wang et al., 2021), causing a spatial variation of soil HMs in different study areas.

3.2. Levels of soil HMs contamination

I_{geo}, PI and PLI of soil HMs were further calculated to explore the contamination status of the study area, and to better distinguish HMs from anthropogenic activities and natural provenance (Fig. 2). The average I_{geo} of the HMs ranged between −0.47 and 0.83, and followed the order Hg (0.83) = Cd (0.83) > Cu (−0.19) > Pb (−0.28) > Ni (−0.29) > As (−0.47). Accordingly, the I_{geo} of Cd and Hg were higher than one (1) in 40% and 56.7% of soil samples, respectively; indicating that Cd and Hg presented low to moderate contamination in the soil of the study area. Nonetheless, the I_{geo} values of the other HMs in more than 85% of all soil samples were lower than zero, suggesting these elements could create negligible contamination in the soil of Yongcheng.

The mean PI values of the soil HMs followed the order: Hg (3.24) > Cd (2.74) > Cu (1.34) > Pb (1.24) = Ni (1.24) > As (1.11). The PI of Cd and Hg were higher than two in more than 70% of the soil samples, denoting an obvious Cd and Hg pollution of the soil in the study area. Moreover, the PLI ranged between 1 and 2 in 90% soil samples, which confirmed the study area was moderately polluted by HMs. The findings of I_{geo}, PI and PLI indicate anthropogenic inputs and pollution by HMs (especially Cd and Hg) in both urban and suburban areas of Yongcheng. Previous research similarly reported anthropogenic effect and HMs pollution in typical coal mine cities in China such as Lianyuan and Tangshan (Liang et al., 2017; Sun et al., 2019).

Table 1
Descriptive statistics of soil HMs concentrations (mg kg^{-1}) in Yongcheng, China.

HMs	Yongcheng City (n = 30)					Urban areas (n = 16)					Suburban areas (n = 14)					BVs
	Max	Min	Mean	SD	CV/%	Max	Min	Mean	SD	CV/%	Max	Min	Mean	SD	CV/%	
Cu	44.46	19.58	26.41	5.19	19.64	44.46	21.61	29.29	5.41	18.48	26.37	19.58	23.13	2.11	9.14	19.7
Ni	42.07	21.15	33.14	4.87	14.71	42.07	31.62	35.91	3.69	10.28	36.91	21.15	29.96	4.11	13.73	26.7
Pb	31.72	18.30	24.36	3.42	14.05	31.72	21.30	26.10	3.25	12.44	27.68	18.30	22.38	2.46	10.99	19.6
Cd	0.29	0.12	0.19	0.05	23.85	0.29	0.16	0.22	0.04	16.16	0.21	0.12	0.16	0.03	17.17	0.07
As	18.30	7.65	12.60	2.57	20.37	18.30	7.65	13.47	2.80	20.79	15.02	8.15	11.60	1.90	16.42	11.4
Hg	0.21	0.01	0.10	0.05	52.31	0.17	0.03	0.11	0.05	43.16	0.21	0.01	0.08	0.05	63.84	0.03

SD: standard deviation; CV: coefficient of variation.
BVs: background values derived from CNEMC (1990).

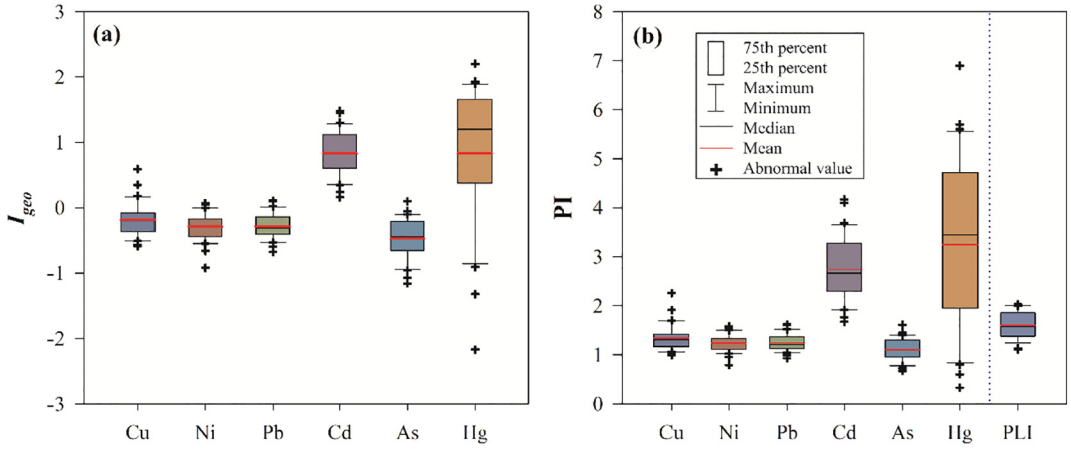

Fig. 2. Contamination characteristics of soil HMs in Yongcheng: (a) Geo-accumulation index (I_{geo}), (b) Pollution Index (PI) and Pollution Load Index (PLI).

3.3. Source apportionment of soil HMs

This study used the PMF 5.0 model to identify and assign sources of soil HMs in Yongcheng. Four factors solutions were determined based on the minimum and stable Q values, at which time most of the residual was ranged from −4 to 4. The signal-to noise ratios (S/N) were greater than 8 and categorized as strong, which ensured the rationality of this model (Luo et al., 2022). Moreover, the model highly predicted the high measured data of each HM, with coefficient of determinations (r^2) higher than 0.80, except for Ni (r^2 = 0.67) and Pb (r^2 = 0.73). This finding indicates that the PMF model parameters are chosen reasonably and the results are reliable (Luo et al., 2022). Thus, this model would be appropriate to explain the sources of soil HMs in the study area.

The detailed depiction of the factor profiles and contribution of each HM by PMF model showed that the first factor (Factor 1) accounted for 27.7% of the contribution, with As (27.2%), Pb (25.9%) and Ni (30.3%) having higher factor loads than the other HMs (Fig. 3). As shows the distribution of Factor 1 (Fig. 4), the sites with high-value concentrated around the urban center and southeast part of the study area. This finding was consistent with the distributing patterns of As, Pb and Ni concentrations, where high accumulations of these HMs were recorded near the same locations (Fig. S1). Generally, As and Ni are regarded as indicators of natural origin, and are widely present in soil parental materials and pedogenic processes (Jin et al., 2019; Huang et al., 2021). Meanwhile, As and Ni could be recognized as natural origins because their average contents were very close to their corresponding BVs (Huang et al., 2021). Therefore, Factor 1 might be related to natural sources.

The second and highest factor accounted for 33.4% of the contribution and displayed high loadings (over 30%) for all HMs, except for Hg. The spatial distribution of Factor 2 dominated the northeastern and western parts of the study area, which showed strong effects on the concentrations of soil HMs (Figs. 4 and S1). High concentrations of Pb, Cd and Cu accumulated in the urban areas with the most serious traffic pollution, because the city center commonly reflects greater traffic volume (Huang et al., 2021). The main sources of soil Pb, Cd and Cu pollution are engine wear, leaded gasoline, braking, and other sources of traffic, which could be released, then deposited and adsorbed into the environment (Men et al., 2020; Huang et al., 2021). The main sources of Pb emissions from vehicles are wear and tear rather than fuel combustion, although trace amounts of Pb remain in many fuels since leaded gasoline was phased out in recent years (Luo et al., 2022). Hence, Factor 2 might be assigned to traffic emissions.

The third factor (Factor 3) explained 16.2% of the contribution, and presented the highest loadings of Hg (60.5%) (Fig. 3). As above-mentioned, several sampling sites exhibited obvious Hg pollution in soils of the study area. Hg had the highest pollution level according to I_{geo} and PI results (Fig. 2), indicating that the accumulation of soil Hg originated mainly from anthropogenic sources. The main source of soil Hg contamination is the application of pesticides and fertilizers containing Hg, which are widely used and overused in agricultural activities (Men et al., 2020; Huang et al., 2021). The highest concentrations of soil Hg mainly occurred in urban center and southeastern parts of the study area, and coincided with the spatial distribution pattern of Factor 3 (Fig. 4). Hg contained in pesticides and fertilizers could be released into the environment and become concentrated in

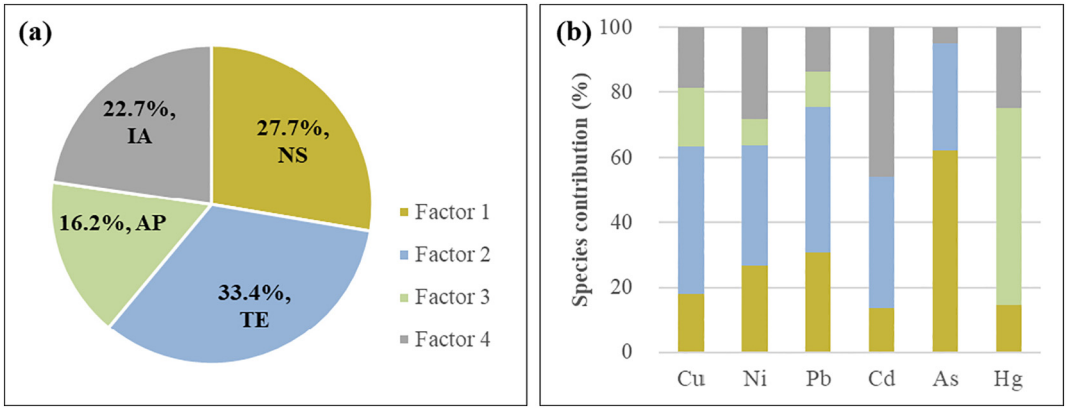

Fig. 3. Source apportionment of soil HMs in Yongcheng, China. (a) Contribution of each factor (NS: natural sources; TE: traffic emissions; AP: agricultural practices; IA: industrial activities). (b) factor profiles of soil HMs.

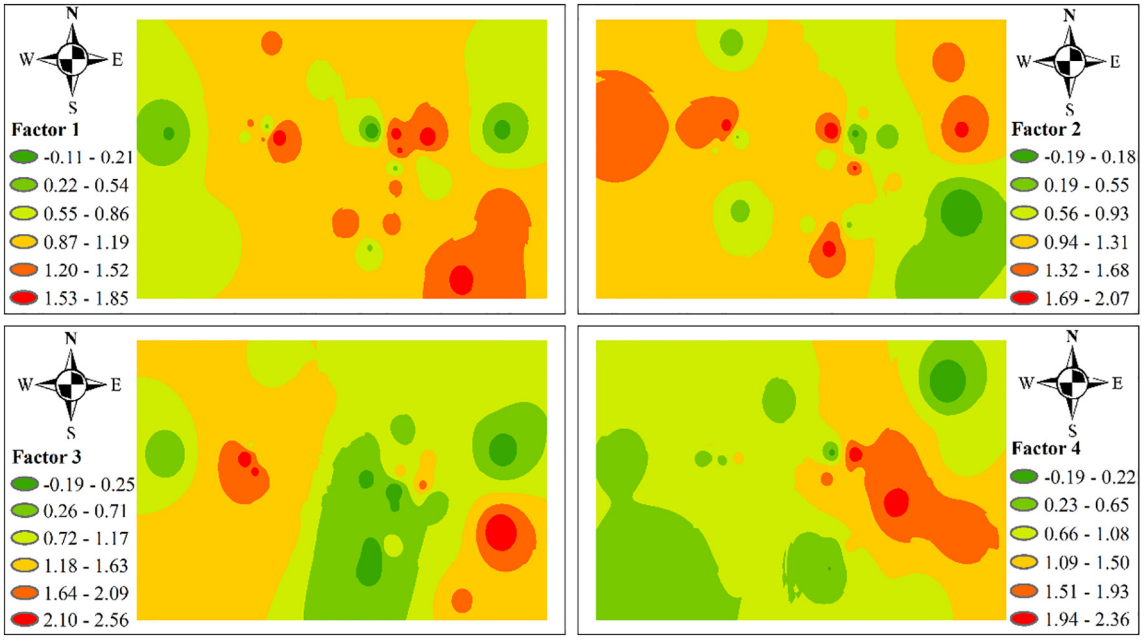

Fig. 4. Spatial distribution of four factors (factor 1 to 4: natural sources, traffic emissions, agricultural practices and industrial activities, respectively) in Yongcheng, China.

surface soils due to its high volatility and migration (Cheng et al., 2020). Hence, the long-term application of agro-chemicals and livestock manures might lead to Hg contamination in the study area; and the Factor 3 can therefore be derived from agricultural practices.

Finally, Factor 4 accounted for 22.7% of the contribution with high loadings of Cd (45.8%), Ni (28.3%), and Hg (24.9%) (Fig. 3). The soils in the study area showed a serious pollution level by Cd and Hg (Fig. 2), indicating significant effects from anthropogenic activities (Men et al., 2020). Previous research highlighted a significant amount of Cd releases from coal-related industrial activities, mostly through coal (Huang et al., 2021; Luo et al., 2022). Coal resource development and combustion are generally important sources of environmental Hg releases, with relatively high content of Hg (about 0.17 mg kg^{-1}) in coal in China (Zhang et al., 2012). Burning coal releases Hg into the atmosphere, which can then be deposited on the soil by atmospheric deposition (Jiang et al., 2020). The sites with high Hg and Cd contents were located in the southeast of the study area (Fig. S1), especially due to the rapid development of industrial activities in the eastern area. In fact, there are several industrial parks founded on the east of the study area (egg. a large in-use coal mine), and they consume large amounts of coal for their activities. Hence, Factor 4 was identified as industrial activities.

3.4. Source-specific quantification of potential ecological risk

Here, potential ecological risk (RI) assessment method was first adopted to assess the ecological risk levels of soil HMs in the study area. Then, we used the PMF model to disassemble and evaluate the RI contributed by the above four sources. The average E_r for each HMs followed the order Hg (129.8) > Cd (82.3) > As (11.1) > Cu (6.7) > Ni (6.2) > Pb (1.2). The average RI in the urban and suburban sites were 237.3 and 267.8, respectively (Table 2), indicating a moderate level of the ecological risk in the study area. Most areas with high-values of RI were located close to the urban center and southeast of the city, showing that urban activities caused severe damage to local ecological environment (see Fig. 5).

Table 2 lists the potential ecological risks associated with soil HMs from four identified sources. In the urban area, contributions from four sources ranged in the following order: industrial activities > agricultural practices > natural source > traffic emission (Table 2). This result indicates that the source from industrial activities was the leading contribution of ecological risk in the urban area. Meanwhile, the highest contribution to ecological risk in the suburban area was from agricultural practices, followed by natural sources, traffic emissions and industrial activities (Table 2). These findings can also be attributed to the loadings of HMs (Hg, Cd) released by industrial activities in urban areas and agricultural practices (Hg) in suburban areas were higher than those from the other sources (Jiang et al., 2020).

3.5. Source-specific quantification of human health risk

Health risk assessment (HHR) of soil HMs to adults and children has become a hotspot in the last years (Huang et al., 2021; Men et al., 2021). PMF-based HHR model was used to quantify the non-carcinogenic and carcinogenic risks associated with soil HMs exposure from various sources (Jiang et al., 2020). According to the soil HM exposure model, ADIs under the ingestion, inhalation, and dermal absorption routes were

Table 2
Potential ecological risk of soil HMs from different sources in Yongcheng, China.

	Factor 1 Natural sources	Factor 2 Traffic emissions	Factor 3 Agricultural practices	Factor 4 Industrial activities	Total factors
Urban areas	63.94	60.91	65.29	77.62	267.75
Proportion (%)	23.88	22.75	24.38	28.99	–
Suburban areas	54.23	50.28	56.99	40.92	202.43
Proportion (%)	26.79	24.84	28.16	20.21	–
Yongcheng	59.41	55.95	61.42	60.49	237.27
Proportion (%)	25.04	23.58	25.89	25.49	–

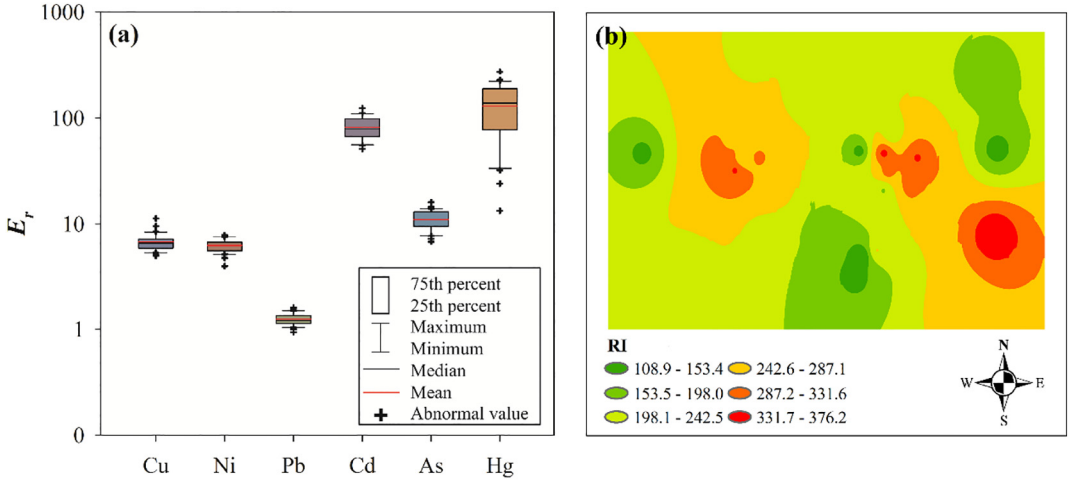

Fig. 5. Computed potential ecological risk factor (E_r) and spatial distribution of potential ecological risk (RI).

calculated, and followed the order $ADI_{ingestion} > ADI_{dermal} > ADI_{inhalation}$ (Table S4). As a result, ingestion was the most important route of soil HMs effects on human health.

Children were more vulnerable to non-carcinogenic risk than adults as the THI was higher for children than adults (Table 3). The THIs of both adults and children were less than one in urban and suburban sites, which reveals no obvious non-carcinogenic risk for residents in the study area (Fig. 6). For the carcinogenic risk, the values of TCR for adults and children were within the range of 1E−06 and 1E−04, suggesting a limited tolerable carcinogenic risks and hazards to human health. Both the carcinogenic and non-carcinogenic risks were significantly higher for children compared to adults (Table 3). This might be explained by child-specific physiological and behavior patterns, since children have more extensive hand-to-mouth behaviors than the adults (Men et al., 2020). Finally, both the THI and TCR exhibited the same distribution pattern, with higher risk in urban area than that of the suburban area.

The contribution orders of four factors to non-carcinogenic risk were similar for both adults and children, and ranged in the order traffic emissions > natural source > agricultural practices > industrial activities. In fact, traffic activities and natural origin mostly contributed to non-carcinogenic risk, because these sources mainly emitted As that posed more than 80% of the total non-carcinogenic risk among the six HMs (Table 3). However, the concentration of As in the study area was similar to its corresponding BV, and showed no obvious pollution level (Table 1, Fig. 2). This result indicates that the most contributing HMs to the non-carcinogenic risk were different from those leading to higher pollution such as Cd and Hg. For the carcinogenic risk, the most contributing factor was also traffic emissions, followed by natural source, industrial activities and agricultural practices, respectively (Table 3). Ni and As (Ni > As) mainly contributed to carcinogenic risk compared to the other HMs due to their very high *SF* for inhalation, ingestion and dermal absorption routes (Heidari et al., 2021). These two HMs together constituted more than 95% of the total carcinogenic risk in the study area, with high loadings in natural source and traffic emissions. In this regard, the carcinogenic risk profiles were mainly affected by As concentrations attributed to each factor, not by the concentration profiles presented in Fig. 3. Hence, the high non-carcinogenic toxicity of As, and the high carcinogenicity of As and Ni have mainly changed the source-specific health risk profiles relative to the concentration profiles in the study area (Heidari et al., 2021).

3.6. Limitations of this study

This study assessed HMs contamination in a typical coal mine city of central China, and quantified source-specific ecological and health risks through an integrated approach. However, this study has some limitations. First, it only focused on the hazards of six HMs (Cu, Ni, Pb, Cd, As and Hg) in surface soils, but other HMs, such as Zn and Cr, that may be hazardous to human health were not included. Second, information on soil properties such as pH, organic matter content, and particle size, etc., from the samples was missing. The physical and chemical properties of soils have critical

Table 3
Human health risks of soil HMs from different sources in Yongcheng, China.

	Children					Adults				
	Factor 1 Natural source	Factor 2 Traffic emission	Factor 3 Agricultural practices	Factor 4 Industrial activities	Total factors	Factor 1 Natural source	Factor 2 Traffic emission	Factor 3 Agricultural practices	Factor 4 Industrial activities	Total factors
Non-carcinogenic risk (HI)										
Cu	2.01E−03	2.47E−03	2.00E−03	2.02E−03	8.51E−03	2.17E−04	2.66E−04	2.16E−04	2.18E−04	9.17E−04
Ni	5.25E−03	5.90E−03	4.87E−03	5.34E−03	2.14E−02	5.66E−04	6.36E−04	5.25E−04	5.76E−04	2.30E−03
Pb	2.20E−02	2.62E−02	2.08E−02	2.14E−02	9.04E−02	2.38E−03	2.84E−03	2.25E−03	2.32E−03	9.79E−03
Cd	7.29E−04	8.55E−04	6.51E−04	8.02E−04	3.04E−03	8.83E−05	1.04E−04	7.89E−05	9.72E−05	3.68E−04
As	1.42E−01	1.44E−01	1.23E−01	1.30E−01	5.40E−01	1.53E−02	1.55E−02	1.33E−02	1.40E−02	5.81E−02
Hg	1.10E−03	8.53E−04	1.26E−03	1.08E−03	4.29E−03	1.21E−04	9.35E−05	1.38E−04	1.18E−04	4.70E−04
THI	1.73E−01	1.80E−01	1.53E−01	1.61E−01	6.68E−01	1.86E−02	1.94E−02	1.65E−02	1.74E−02	7.19E−02
Carcinogenic risk (CR)										
Ni	1.61E−05	1.81E−05	1.49E−05	1.63E−05	6.54E−05	7.15E−06	8.04E−06	6.63E−06	7.27E−06	2.91E−05
Pb	5.52E−08	6.58E−08	5.22E−08	5.37E−08	2.27E−07	2.37E−08	2.82E−08	2.24E−08	2.30E−08	9.73E−08
Cd	2.77E−08	3.25E−08	2.47E−08	3.05E−08	1.15E−07	1.26E−08	1.48E−08	1.12E−08	1.38E−08	5.24E−08
As	5.48E−06	5.56E−06	4.76E−06	5.03E−06	2.08E−05	2.36E−06	2.40E−06	2.05E−06	2.17E−06	8.97E−06
TCR	2.16E−05	2.37E−05	1.97E−05	2.15E−05	8.66E−05	9.55E−06	1.05E−05	8.72E−06	9.48E−06	3.82E−05

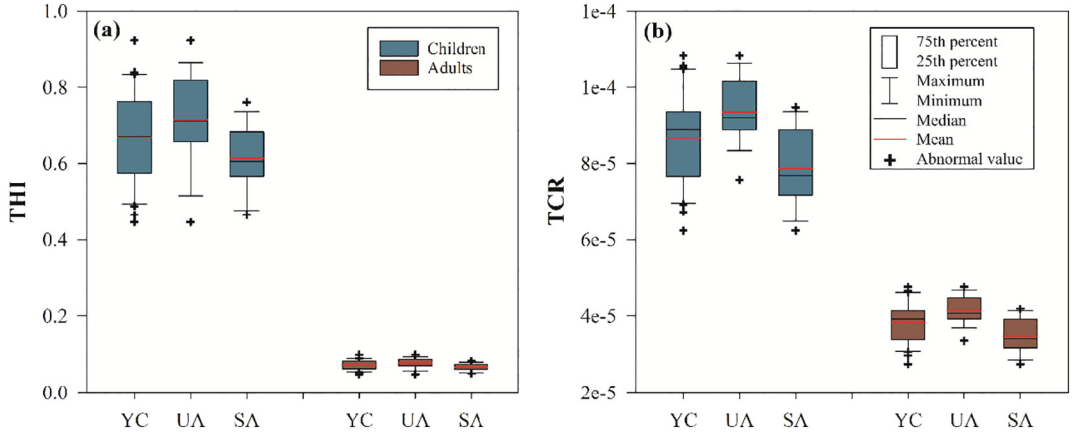

Fig. 6. Non-carcinogenic risks (THI) and carcinogenic risks (TCR) posed by soil HMs for children and adults in Yongcheng (YC), urban areas (UA) and suburban areas (SA).

effects on the availability, distribution and concentration of HMs (Huang et al., 2021). Therefore, future research should pay close attention on the status of more HMs and the soil properties, so that the assessment bias on subsequent risks analysis can be reduced. Meanwhile, more focus should be strengthened on the integration of different methods to accurately evaluate and validate the source apportionment results.

4. Conclusions

In this study, we investigated the soil HMs contamination and pollution sources in a typical coal industrial city. The ecological and human health risks from specific sources were also quantitatively evaluated through an integrated approach. Overall, the average concentrations of HMs exceeded the corresponding BVs, and the study area was moderately contaminated by soil HMs, especially from the accumulation of Cd and Hg. HMs pollution was higher for soils in urban area than soils suburban area. The specific contributions of four sources, including natural source, traffic emissions, agricultural practices and industrial activities, were apportioned as 27.7%, 33.4%, 16.2% and 22.7%, respectively. The ecological and human health risks from PMF-based RI and HHR models were quantified from four source factors; and a moderate ecological risk occurred in the whole study area, with industrial activities and agricultural practices as leading contributions in the urban and suburban areas, respectively. The non-carcinogenic risks for both adults and children were lower than the risk threshold, while the carcinogenic risks were within the range of 1E−06 and 1E−04, suggesting that carcinogenic risks and hazards to human health should not be neglected. In addition, the non-carcinogenic and carcinogenic risks of children were higher than those of adults, while the contributions of human health risk from different sources were very similar between the two groups. Sources from traffic emissions and natural origin mainly contributed to the non-carcinogenic and carcinogenic risks in the study area, due to the high non-carcinogenicity and carcinogenicity of As and Ni. These findings suggest that the combination of risk assessment models and PMF can be an effective method in obtaining accurate source apportionment of soil HMs; and the results are of great significance for decision-makers to reduce ecological and human health risks from potential contamination sources.

CRediT authorship contribution statement

Xian-Meng Shi: Conceptualization, Software, Writing-original draft, Funding acquisition. **Shuai Liu**: Investigation, Writing - review & editing, Funding acquisition. **Liang Song**: Methodology, Writing - review & editing, Supervision, Funding acquisition. **Chuan-Sheng Wu**: Visualization, Investigation. **Bin Yang**: Software, Writing - review & editing. **Hua-Zheng Lu**: Data curation, Validation. **Xun Wang**: Validation, Writing - review & editing. **Sissou Zakari**: Visualization, Writing - review & editing.

Declaration of competing interest

The authors declare that they have no known competing financial interests or personal relationships that could have appeared to influence the work reported in this paper.

Acknowledgment

This work was funded by the Natural Science Foundation of Henan Province (222300420257), the Scientific Startup Foundation for Doctors of Shangqiu Normal University (700170), the National Natural Science Foundation of China (32171529), the Yunnan Natural Science Foundation (202101AT070059), the Candidates of the Young and Middle Aged Academic Leaders of Yunnan Province (2019HB040), the Yunnan High Level Talents Special Support Plan (YNWR-QNBJ-2020-066), and the Natural Science Foundation of Universities of Anhui Province (KJ2020A0095). We thank Mr. Yu-Xuan Mo for his constructive suggestions to improve the quality of the graphical abstract.

Appendix A. Supplementary data

Supplementary data to this article can be found online at https://doi.org/10.1016/j.scitotenv.2022.155694.

References

Briffa, J., Sinagra, E., Blundell, R., 2020. Heavy metal pollution in the environment and their toxicological effects on humans. Heliyon 6, e04691. https://doi.org/10.1016/j.heliyon.2020.e04691.

Cao, C., Zhang, Q., Ma, Z.-B., Wang, X.-M., Chen, H., Wang, J.-J., 2018. Fractionation and mobility risks of heavy metals and metalloids in wastewater-irrigated agricultural soils from greenhouses and fields in Gansu, China. Geoderma 328, 1–9. https://doi.org/10.1016/j.geoderma.2018.05.001.

Cheng, W., Lei, S., Bian, Z., Zhao, Y., Li, Y., Gan, Y., 2020. Geographic distribution of heavy metals and identification of their sources in soils near large, open-pit coal mines using positive matrix factorization. J. Hazard. Mater. 387, 121666. https://doi.org/10.1016/j.jhazmat.2019.121666.

CNEMC, 1990. Soil Elements Background Values in China. Environmental Science Press of China, Beijing China National Environmental Monitoring Centre.

Cui, X., Wang, X., Liu, B., 2020. The characteristics of heavy metal pollution in surface dust in Tangshan, a heavily industrialized city in North China, and an assessment of associated health risks. J. Geochem. Explor. 210. https://doi.org/10.1016/j.gexplo.2019.106432.

Gu, Y.G., Gao, Y.P., 2018. Bioaccessibilities and health implications of heavy metals in exposed-lawn soils from 28 urban parks in the megacity Guangzhou inferred from an in vitro physiologically-based extraction test. Ecotoxicol. Environ. Saf. 148, 747–753. https://doi.org/10.1016/j.ecoenv.2017.11.039.

Guan, Q., Wang, F., Xu, C., Pan, N., Lin, J., Zhao, R., Yang, Y., Luo, H., 2018. Source apportionment of heavy metals in agricultural soil based on PMF: a case study in Hexi Corridor, northwest China. Chemosphere 193, 189–197. https://doi.org/10.1016/j.chemosphere.2017.10.151.

Guo, G., Zhang, D., Yuntao, Wang, 2021. Source apportionment and source-specific health risk assessment of heavy metals in size-fractionated road dust from a typical mining

and smelting area, Gejiu, China. Environ. Sci. Pollut. Res. 28, 9313–9326. https://doi.org/10.1007/s11356-020-11312-y.
Han, R., Zhou, B., Huang, Y., Lu, X., Li, S., Li, N., 2020. Bibliometric overview of research trends on heavy metal health risks and impacts in 1989–2018. J. Clean. Prod. 276. https://doi.org/10.1016/j.jclepro.2020.123249.
Heidari, M., Darijani, T., Alipour, V., 2021. Heavy metal pollution of road dust in a city and its highly polluted suburb; quantitative source apportionment and source-specific ecological and health risk assessment. Chemosphere 273, 129656. https://doi.org/10.1016/j.chemosphere.2021.129656.
Hossen, M.A., Chowdhury, A.I.H., Mullick, M.R.A., Hoque, A., 2021. Heavy metal pollution status and health risk assessment vicinity to Barapukuria coal mine area of Bangladesh. Environ. Nano. Monit. Manag. 16. https://doi.org/10.1016/j.enmm.2021.100469.
Huang, J., Guo, S., Zeng, G.M., Li, F., Gu, Y., Shi, Y., Shi, L., Liu, W., Peng, S., 2018. A new exploration of health risk assessment quantification from sources of soil heavy metals under different land use. Environ. Pollut. 243, 49–58. https://doi.org/10.1016/j.envpol.2018.08.038.
Huang, Y., Wang, L., Wang, W., Li, T., He, Z., Yang, X., 2019. Current status of agricultural soil pollution by heavy metals in China: a meta-analysis. Sci. Total Environ. 651, 3034–3042. https://doi.org/10.1016/j.scitotenv.2018.10.185.
Huang, J., Wu, Y., Sun, J., Li, X., Geng, X., Zhao, M., Sun, T., Fan, Z., 2021. Health risk assessment of heavy metal(loid)s in park soils of the largest megacity in China by using Monte Carlo simulation coupled with positive matrix factorization model. J. Hazard. Mater. 415, 125629. https://doi.org/10.1016/j.jhazmat.2021.125629.
Ji, H., Li, H., Zhang, Y., Ding, H., Gao, Y., Xing, Y., 2017. Distribution and risk assessment of heavy metals in overlying water, porewater, and sediments of Yongding River in a coal mine brownfield. J. Soils Sediments 18, 624–639. https://doi.org/10.1007/s11368-017-1833-y.
Jiang, Y., Chao, S., Liu, J., Yang, Y., Chen, Y., Zhang, A., Cao, H., 2017. Source apportionment and health risk assessment of heavy metals in soil for a township in Jiangsu Province, China. Chemosphere 168, 1658–1668. https://doi.org/10.1016/j.chemosphere.2016.11.088.
Jiang, H.H., Cai, L.M., Wen, H.H., Hu, G.C., Chen, L.G., Luo, J., 2020. An integrated approach to quantifying ecological and human health risks from different sources of soil heavy metals. Sci. Total Environ. 701, 134466. https://doi.org/10.1016/j.scitotenv.2019.134466.
Jin, Y., O'Connor, D., Ok, Y.S., Tsang, D.C.W., Liu, A., Hou, D., 2019. Assessment of sources of heavy metals in soil and dust at children's playgrounds in Beijing using GIS and multivariate statistical analysis. Environ. Int. 124, 320–328. https://doi.org/10.1016/j.envint.2019.01.024.
Lei, M., Zhang, Y., Khan, S., Qin, P.F., Liao, B.H., 2010. Pollution, fractionation, and mobility of Pb, Cd, Cu, and Zn in garden and paddy soils from a Pb/Zn mining area. Environ. Monit. Assess. 168, 215–222. https://doi.org/10.1007/s10661-009-1105-4.
Li, Z., Ma, Z., van der Kuijp, T.J., Yuan, Z., Huang, L., 2014. A review of soil heavy metal pollution from mines in China: pollution and health risk assessment. Sci. Total Environ. 468–469, 843–853. https://doi.org/10.1016/j.scitotenv.2013.08.090.
Liang, J., Feng, C., Zeng, G., Gao, X., Zhong, M., Li, X., Li, X., He, X., Fang, Y., 2017. Spatial distribution and source identification of heavy metals in surface soils in a typical coal mine city, Lianyuan, China. Environ. Pollut. 225, 681–690. https://doi.org/10.1016/j.envpol.2017.03.057.
Liu, X., Bai, Z., Shi, H., Zhou, W., Liu, X., 2019. Heavy metal pollution of soils from coal mines in China. Nat. Hazards 99, 1163–1177. https://doi.org/10.1007/s11069-019-03771-5.
Liu, X., Shi, H., Bai, Z., Zhou, W., Liu, K., Wang, M., He, Y., 2020. Heavy metal concentrations of soils near the large opencast coal mine pits in China. Chemosphere 244, 125360. https://doi.org/10.1016/j.chemosphere.2019.125360.
Lu, C., Wang, S., Wang, K., Gao, Y., Zhang, R., 2020. Uncovering the benefits of integrating industrial symbiosis and urban symbiosis targeting a resource-dependent city: a case study of Yongcheng, China. J. Clean. Prod. 255. https://doi.org/10.1016/j.jclepro.2020.120210.
Luo, H., Wang, Q., Guan, Q., Ma, Y., Ni, F., Yang, E., Zhang, J., 2022. Heavy metal pollution levels, source apportionment and risk assessment in dust storms in key cities in Northwest China. J. Hazard. Mater. 422, 126878. https://doi.org/10.1016/j.jhazmat.2021.126878.
Mahato, M.K., Singh, G., Singh, P.K., Singh, A.K., Tiwari, A.K., 2017. Assessment of mine water quality using heavy metal pollution index in a coal mining area of Damodar River Basin, India. Bull. Environ. Contam. Toxicol. 99, 54–61. https://doi.org/10.1007/s00128-017-2097-3.
Men, C., Liu, R., Wang, Q., Guo, L., Shen, Z., 2018. The impact of seasonal varied human activity on characteristics and sources of heavy metals in metropolitan road dusts. Sci. Total Environ. 637–638, 844–854. https://doi.org/10.1016/j.scitotenv.2018.05.059.
Men, C., Liu, R., Xu, L., Wang, Q., Guo, L., Miao, Y., Shen, Z., 2020. Source-specific ecological risk analysis and critical source identification of heavy metals in road dust in Beijing, China. J. Hazard Mater. 388, 121763. https://doi.org/10.1016/j.jhazmat.2019.121763.
Men, C., Wang, Y., Liu, R., Wang, Q., Miao, Y., Jiao, L., Shoaib, M., Shen, Z., 2021. Temporal variations of levels and sources of health risk associated with heavy metals in road dust in Beijing from May 2016 to April 2018. Chemosphere 270, 129434. https://doi.org/10.1016/j.chemosphere.2020.129434.
Norris, G.A., Duvall, R., Brown, S.G., Bai, S., 2014. EPA Positive Matrix Factorization (PMF) 5.0 Fundamentals and User Guide. U.S. Environmental Protection Agency, Office of Research and Development, Washington, DC, 20460.
Ren, Y., Luo, Q., Zhuo, S., Hu, Y., Shen, G., Cheng, H., Tao, S., 2021. Bioaccessibility and public health risk of heavy metal(loid)s in the airborne particulate matter of four cities in northern China. Chemosphere 277, 130312. https://doi.org/10.1016/j.chemosphere.2021.130312.
Sun, L., Guo, D., Liu, K., Meng, H., Zheng, Y., Yuan, F., Zhu, G., 2019. Levels, sources, and spatial distribution of heavy metals in soils from a typical coal industrial city of Tangshan, China. Catena 175, 101–109. https://doi.org/10.1016/j.catena.2018.12.014.
Tchounwou, P.B., Yedjou, C.G., Patlolla, A.K., Sutton, D.J., 2012. Heavy metal toxicity and the environment. Exp. Suppl. 101, 133–164. https://doi.org/10.1007/978-3-7643-8340-4_6.
USEPA, 2014. EPA Positive Matrix Factorization (PMF) 5.0 Fundamentals and User Guide. https://www.epa.gov/sites/production/files/2015-02/documents/pmf_5.0_user_guide.pdf.
Wang, H.-Z., Cai, L.-M., Wang, Q.-S., Hu, G.-C., Chen, L.-G., 2021. A comprehensive exploration of risk assessment and source quantification of potentially toxic elements in road dust: a case study from a large Cu smelter in central China. Catena 196. https://doi.org/10.1016/j.catena.2020.104930.
Zhang, L., Wang, S., Meng, Y., Hao, J., 2012. Influence of mercury and chlorine content of coal on mercury emissions from coal-fired power plants in China. Environ. Sci. Technol. 46, 6385–6392. https://doi.org/10.1021/es300286n.
Zhang, P., Qin, C., Hong, X., Kang, G., Qin, M., Yang, D., Pang, B., Li, Y., He, J., Dick, R.P., 2018. Risk assessment and source analysis of soil heavy metal pollution from lower reaches of Yellow River irrigation in China. Sci. Total Environ. 633, 1136–1147. https://doi.org/10.1016/j.scitotenv.2018.03.228.